Coherent Soft X-Ray Imaging and Diffraction

(CSXID)

A new UK capability for functional and quantum materials research

Prepared for the **Diamond SAC/DISCo**

November 2020

1. Acknowledgements

The CSXID beamline User Working Group (UWG) members are:

Paolo Radaelli (**Chair**)	University of Oxford
Claire Donnelly	University of Cambridge
Massimo Ghidini	University of Cambridge/Parma and Diamond Light Source
Kevin Edmonds (**DUC**)	University of Nottingham
Jörg Wunderlich	University of Regensburg
Andy Beale	University College London
Olga Kazakova (**DISCo**)	National Physical Laboratory
Robert Weatherup	University of Oxford
Benedikt Daurer	Diamond Light Source
Burkhard Kaulich	Diamond Light Source
Dirk Backes	Diamond Light Source
Hongchang Wang	Diamond Light Source
Martin Burt	Diamond Light Source
Sarnjeet Dhesi (**Diamond lead**)	Diamond Light Source

Larissa Ishibe-Veiga contributed to the science case for this proposal.

A Quantum Materials workshop was held at Cosener's House in September 2018 which identified a versatile polarised soft X-ray imaging beamline as a key requirement of the community.

The UWG Zoom meetings were held on the 30th September, 23rd October and 10th November 2020.

A communication and engagement webinar was held on the 28th October 2020 with 147 registered participants and 103 attendees. Thanks to Emily Baird, from the Diamond Communications Group, who organised the webinar.

An email summarising the question and answer session discussions during the webinar was distributed to the registrants on the 6th November 2020.

The CSXID beamline UWG thanks the user community for the numerous conversations and comments during the preparation of this proposal.

2. Executive Summary

There is currently a global effort to understand and control the physical properties of functional and quantum materials, with the promise of next-generation low-cost, energy-efficient devices. The UK is a world leader in this endeavour, but there is an urgent need to develop new, multidisciplinary and multidimensional tools to understand nanoscale emergent complexity if the UK is to remain competitive. The dramatic increase in coherent flux on Diamond-II will revolutionise our ability to explore the static and dynamic 3D properties of a whole range of materials from emergent quantum materials to materials already used in applications, such as composite battery electrodes and nanocatalysts. We propose to add a new, cutting-edge capability to the UK science base by constructing a world-leading beamline for Coherent Soft X-ray Imaging and Diffraction (CSXID) with advanced sample environments. The beamline will take full advantage of the increased coherent flux on Diamond-II, dramatically improving the spatial resolution, for an array of coherent X-ray imaging probes, whilst significantly reducing the time to record 3D tomograms. The CSXID beamline will then enable UK science and industry with a new suite of fully automated, polarised X-ray tools (*e.g.* Ptychography, Bragg Coherent Diffraction Imaging, NanoDiffraction Imaging, Fourier-Transform Holography) providing unprecedented insights relating nanoscale 3D structure directly to function.

The new CSXID beamline is a timely contribution to the Diamond-II upgrade and will transform many UK research fields through rapid, nanoscale 3D imaging of the chemical and physical processes critical to the development of, for instance, secure low-energy data-storage materials, battery materials and quantum materials. The scientific advances enabled are key to the UK Industrial Strategy[a], UK National Quantum Technologies Programme[b], Faraday Institution[c], Royce Institute[d] and EPSRC grand challenges including Nanoscale Design of Functional Materials and New Quantum Technologies[e].

[a] https://www.gov.uk/government/publications/industrial-strategy-the-grand-challenges/industrial-strategy-the-grand-challenges
[b] https://uknqt.epsrc.ac.uk/
https://iopscience.iop.org/article/10.1088/2058-9565/ab4346/pdf
[c] https://faraday.ac.uk/wp-content/uploads/2018/11/Faraday-Infrastructure-Report.pdf
[d] https://www.royce.ac.uk/materials-for-the-energy-transition/
[e] https://epsrc.ukri.org/research/ourportfolio/vop/pack/THEME/

3. Scientific case

3.1 Introduction

X-ray imaging has resolved a wealth of nanoscale phenomena[1–3] and has underpinned the understanding and development of a vast range of materials used in technological applications. In this respect, realising the full potential of functional and quantum materials requires advanced probes essential for the prediction-production-characterisation (PPC) paradigm of developing new materials with optimised properties for next-generation devices. The transformative research directions outlined in Diamond-II | Advancing Science describe how the increased coherence offered by Diamond-II will unravel some of the fundamental nanoscale interactions governing the physical properties of new materials, aiding methods to design, fabricate and control such materials for future applications. In this section, we present a range of science topics, drawn from key disciplines, highlighting how a new CSXID polarised soft X-ray beamline will have immediate impact on the UK research landscape. The beamline will host a multidisciplinary user community working in diverse areas such as 3D domain mapping and dynamics in ferroic materials, 3D electrochemical reaction tracking and chemical speciation location in battery materials.

3.2 Scientific opportunities enabled by the CSXID beamline

3.2.1 A new dimension for ferroic imaging

The ability to control and manipulate magnetism has been the lynchpin of some of the most important technological advances of the last one hundred years (*e.g.* magnetic resonance imaging, huge data centres, wind turbine electric motors). In terms of magnetic materials, performance is optimised and new functionalities are unlocked when good control of the influence of the material microstructure on the highly inhomogeneous 3D magnetisation vector field is achieved. Macroscopic probes give an average of all material properties and thus deliver, at best, indirect information about the key role of magnetic and microstructural inhomogeneities. In recent years, 2D magnetisation vector maps provided by magnetic microscopy, have revolutionised our understanding of the performance and reliability of thin films devices[2,4,5]. In particular, X-ray based PhotoEmission Electron Microscopy (PEEM) has made significant contributions in this area[6–8], but it is a near surface technique with *in situ* magnetic fields limited to a few mT and a spatial resolution limited to ~10nm using synchrotron X-ray sources.

The CSXID beamline will build on these advances by enabling 3D imaging of ferroic materials at unexplored lengthscales and experimental conditions: ultrahigh 3D spatial resolution (<10 nm) in applied magnetic and electric fields. These unique characteristics will be transformative in a number of important areas. For instance, the Brown paradox[9], *i.e.* nanoscale defects depressing coercivity and thus the energy density that can be stored in permanent magnets[10] is a classical micromagnetic problem. The new imaging capability on the CSXID beamline will enable detailed tracking of magnetisation reversal processes in 3D to reveal how defects pin and release the local magnetisation vector. High-resolution coherent imaging of ferromagnetic (FM) materials will therefore allow the correlation of the magnetization reversal processes (*e.g.* domain nucleation and propagation) with microstructural features, as well as the more elusive dynamical behaviour of less well-studied systems such as antiferromagnets, multiferroics, ferroelectrics, topological matter and materials driven by strong spin-orbit coupling (SOC). The design of sub-micron sized ferroic materials for future microsystem technologies then becomes a real possibility.

3.2.1.1 Ferromagnetism

The historic lack of a 3D probe of the magnetisation vector field means that more than eighty years after the first magnetic imaging experiments, it was only very recently that a first glimpse into the inner workings of a magnetic system, and its behaviour, could be observed through the development of coherent X-ray magnetic nanotomography[11] and pump-probe magnetic laminography[12]. These recent breakthroughs in both hard[12,13] and soft[14] (see Figure 1) X-ray 3D magnetic imaging provide a route to a greater understanding of the processes that govern magnetic reversal or magnetisation dynamics, and therefore promise new developments of more energy-efficient materials. While first demonstrations of these techniques represent a breakthrough in terms of experimental capabilities, until now the achievable spatial

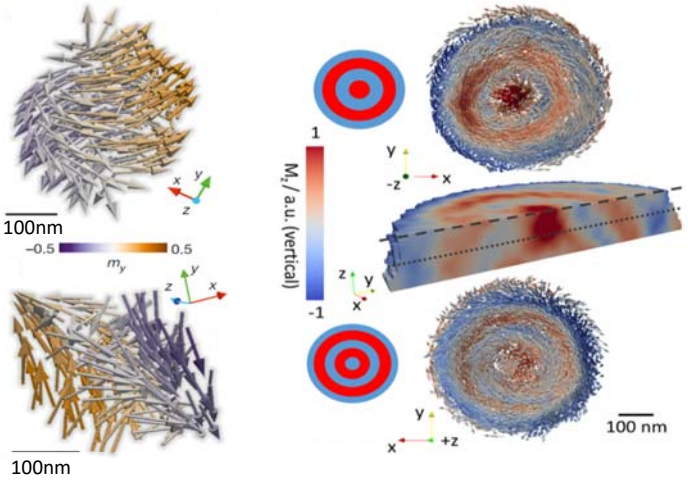

Figure 1 (left - top) Bloch point vortex and (left – bottom) antivortex discovered in $GdCo_2$ using X-ray 3D vector tomography. The arrows represent the local magnetisation vector. See Ref. 11 for details. (right – top) 3D magnetic laminography reconstructions from a 150nm permalloy disc showing the presence of 4 ring domains and a Néel closure cap at the top of the disc, (right-middle) cross-section through the reconstructed volume of the permalloy disc (right-bottom) magnetic structure showing the presence of Bloch domains walls and 5 ring domains at the bottom of the disc. See Ref. 14 for details.

resolution has been far from key material lengthscales, such as the magnetic exchange length, due to weak X-ray Magnetic Circular Dichroism (XMCD) signals in the hard X-ray range used, and the low coherent flux available implying days of data acquisition per 3D reconstruction. In this respect, the increase in coherent flux owing to the upgrade to Diamond-II will provide critical new capabilities to probe complete 3D magnetic profiles under *operando* conditions. In particular, it will give access to key material-specific lengthscales by employing state-of-the-art techniques such as ptychography[11] combined with the laminography geometry[12,14,15] (see section 4.1) using the large XMCD and X-Ray Magnetic Linear Dichroism (XMLD) signals available in the soft and tender X-ray range. These probes will provide both high spatial resolution static imaging, as well as the mapping of picosecond magnetisation dynamics[12] in 3D, allowing tracking of coherent magnetisation rotation, domain wall motion[12] and domain switching in the presence of defects giving unprecedented insights into the behaviour of nanoscale 3D magnetic textures controlling the macroscopic properties of 3*d*, 4*d* and 4*f* materials in which the subtle balance between crystal field effects, bandwidth and SOC lead to a wealth of new phenomena.

Another area with the potential to provide robust and highly functional devices are novel spin textures, which offer enhanced stability and control due to the topology of their states. Indeed, recent demonstrations of controlled motion of chiral spin textures, such as skyrmions[16–24] and domain boundaries in thin films with X-ray magnetic imaging[12,25–38] have provided key insights into the speed of these objects achieved with current pulses. The discovery of skyrmion deflection[14] in nanowires has led to exploration of skyrmion motion in synthetic antiferromagnets which benefits hugely from 2D magnetic imaging[15]. The CSXID beamline will play a major role in the development of high levels of control of the dynamics of these structures by providing an understanding of the distortions and acceleration of chiral spin structures via 3D ultrafast magnetic mapping of the local spin structures with a resolution of <10nm.

The new capabilities of the CSXID beamline also have the potential to drive the development of entirely new fields, such as 3D nanomagnetism, where magnetic materials are sculpted into 3D configurations using advanced nanofabrication techniques[39], leading to exotic properties ranging from magnetochiral structures[40] to ultrafast domain wall motion[41]. This rapidly growing field has the potential to revolutionise storage and information technologies based on the controlled movement of domain wall structures in engineered energy landscapes.

3.2.1.2 Antiferromagnetism

In addition to FM materials, there is growing interest in the rapidly developing field of antiferromagnetic (AFM) spintronics. Initially, the intrinsic high frequencies of AFM dynamics represented the main attraction making AFMs distinct from and advantageous to FMs [Ref. 42]. Later, further interest

was added by the realisation that AFM skyrmions and other topological textures can be created as either stable or metastable objects, and that these would result in a complete cancellation of the Magnus force, resulting in a much better stability in racetrack-type application[43]. Very recently, the so-called AFM 'oxide electronics' came to the fore, employing multi-layers in which the AFM element is an insulating oxide. The AFM oxide can act as a robust 'write' layer that is immune to magnetic fields perturbations, produces no stray-fields, can be switched at ultrafast THz speeds, and is capable of generating large magneto- transport effects[44–47]. Moreover, many oxides of interest have very low damping, leading to the prediction of extremely high skyrmion velocities[48]. A new generation of devices based on AFM spintronics or the hybrid 'oxide electronics + spintronics' approach has immense potential for low-energy post-CMOS electronics.

Soft-X-ray imaging is a powerful tool to study AFM and coupled FM/AFM systems, and much of the relevant work has been carried out at Diamond using XMLD/XMCD-PEEM [Ref. 44,49–51]. A noteworthy development is AFM 'vector-mapping', enabling the full reconstructions of the Néel vector distribution in 2D based on multiple sample rotations using XMLD-PEEM [51]. Electrical switching of AFM ordering was achieved for the first time in 2016 with the aid of 2D magnetic imaging performed at Diamond[44]. This breakthrough in domain switching has received attention from Seagate, Toshiba and Hitachi and has the potential to make inroads into the £32 billion data storage market as well as markets related to secure storage and aviation safety. The work represents the combined strength of predictive theoretical modelling, advanced sample synthesis methods and state-of-the-art X-ray imaging and represents a compelling case for the efficacy of the PPC paradigm.

Understanding the effects of inhomogeneity, defect pinning, magnetostriction and switching using full 3D magnetic imaging will now be key to further develop AFM materials for improved device performance. Recent studies have shown new routes for controlling antiferromagnetism, including magnetoelastic coupling, spin currents, and spin-orbit torques[52]. However, imaging AFM domains in 3D with nanoscale resolution remains elusive, so that the increased coherence of the CSXID beamline will provide a huge boost to the field, stimulating the research and development of powerful new probes combining tomographic methods with XMLD.

3.2.1.3 Multiferroics and ferroelectrics

Magnetic and ferroelectric materials are ubiquitous in the production and transformation of energy, sensing, data storage and biomedicine[10,40,53]. In future, they will continue to enable key technologies that will make the UK economy more efficient, greener and highly automated. Investment in nanoscale ferroic materials will be propelled both by constant market pressure towards miniaturisation and morphological complexity (*e.g.* 3D memory architectures[54]) and by the vast opportunities that physical systems with reduced dimensionality offer for the exploration of novel phenomena[55]. The transition towards nanoferroic devices with complex architectures requires transformative leaps in experimental techniques.

The creation of materials with novel physical properties, predicted by advanced and intensive computational modelling, leads to an immense range of systems that require detailed characterisation to optimise performance. In this respect, one key area of activity is the development of composite materials with multiferroic properties. Naturally occurring multiferroic materials, in which electric fields can control magnetism and vice versa, have intriguing physical properties, but generally exhibit weak coupling even at cryogenic temperatures. On the other hand, thin film composites achieve electrical switching of a substantial net magnetization at room temperature using ferromagnetic thin films in which electrically driven magnetic changes arise due to strain or exchange bias from ferroelectric substrates[8]. New functionalities can also be obtained by stacking layers of different materials in designed heterostructures which can be further enhanced by applying strain[56–59]. However, materials choice, magnetoelectric coefficients and magnitude of applied strain are severely limited by heteroepitaxy (the predominant method to build multilayer stacks) and the inevitable substrate clamping. Recent breakthroughs in the preparations of freestanding stretchable homogeneous[59] and heterogeneous[60] membranes will be

transformative in this field. These methods can be applied to any material with unprecedented extreme strains possible to tune the physical properties and provide a platform for stacking and coupling three-dimensional structures, reminiscent of Van der Waals integration. These systems are naturally suitable for the transmission geometry of laminography and the new CSXID beamline will provide unprecedented insights into magnetoelectric switching, strain, interface coupling and phase separation. Moreover imaging of ferroelectric domain switching in unclamped ferroelectric and magnetoelectric membranes made of composite multiferroics will become possible, using X-ray Linear dichroism as previously demonstrated with PEEM [Ref. 61]. Moreover, the study of topological defects (vortices and skyrmions) in ferroelectric materials, as well as the study of functionalities associated with ferroelectric domain walls, have become a hot topic in the field and would benefit greatly from 3D imaging using laminography.

3.2.2 Spin polarisation in topological insulators

Topological insulators have attracted a great deal of attention in recent years because of their potential applications in spintronics devices, energy-efficient dissipationless circuits and quantum computing. A Topological Insulator (TI) has an insulating bulk and a conducting surface with a Dirac-like band structure[62]. A large SOC together with time reversal symmetry cause the topological nature of these surface states, manifesting itself in the suppression of backscattering and spin-momentum coupling. The latter gives rise to 100% spin-polarised currents, allowing information transport over long distances[63]. Furthermore, magnetic topological insulators exhibit the quantum anomalous Hall (QAH) effect[64,65], characterized by dissipationless chiral currents.

Magnetic dopants in a TI provide an internal magnetic field, allowing the realisation of a quantum Hall-like effect without the need for large magnetic fields or very low temperatures. Transport in the QAH effect[64,65] takes place only at the edges of the sample and is dissipationless, similar to a superconductor. An essential requirement is that the magnetisation is perpendicular to the surface, which in a 3D object such as a nanoribbon is currently not possible to determine. Typical magnetic dopants are transition metals such as Cr and Mn with electronic transitions in the soft X-ray regime. A 3D representation of the dopant-induced magnetisation is then crucial to improve the material properties and advance the understanding of the physics behind the QAH effect. What is more, a doped TI combined with a superconductor leads to Majorana-based circuits; an approach heavily explored for novel quantum computers[66].

The recently discovered spin Hall effect is a means to create pure spin currents, the transport of spin without any net electric charge flowing[67,68]. Remarkably, spin currents create a spin-accumulation in non-magnetic materials[69], essentially instilling magnetic order in a non-magnetic material. A nanoscale level understanding of the detailed spin dependent scattering mechanism is still lacking. Combining STXM, with a detection limit of 10^{-5} μ_B/atom [Ref. 69], and magnetic coherent ptychography/tomography would be a powerful tool that could directly probe the induced spin polarisation with the required resolution. A potential outcome are new concepts for spintronics based entirely on non-magnetic materials.

Bi_2Te_3, Bi_2Se_3 or Sb_2Te_3 exhibit 1D-like chiral states which modify the magnetic landscape considerably due to their 100% spin-polarisation. Modulations in the magnetic order of intrinsic magnetic TI can arise due to atomically sharp terraces (see Figure 2). As a result, domains with FM and AFM order can be found adjacent to each other, harbouring Axion and QAH states adjacent to each other[70]. Ptychography, with its high spatial resolution and sensitivity[71] would be the method of choice to probe the complex modifications and interference effects at the boundary. The new CSXID

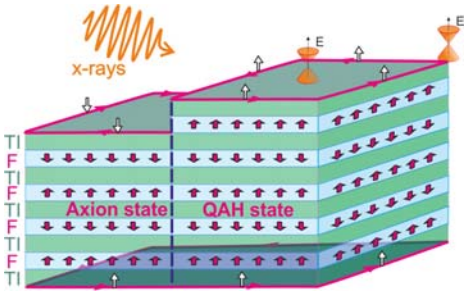

Figure 2 Axion and QAH states in an intrinsic magnetic TI with even and odd number of magnetic layers.

beamline will then offer a crucial new 3D perspective on topological phenomena, in addition to well-established 2D techniques such as nanoARPES and PEEM.

3.2.3 Novel correlated electronic and magnetic states driven by strong spin-orbit coupling

The novel electronic phenomena derived from SOC has opened up several new fields of research, with a prominent example being correlated quantum materials with strong SOC[72,73]. Unlike topological insulators[62] or spin-orbitronics[74] materials, in which the electron states are essentially non-interacting, such systems present partially filled 4*d* or 5*d* orbitals and are heavily influenced by electron-electron correlations[75]. In the limit of strong correlations, SOC can lift the degeneracy of partially filled *d*-shells providing a mechanism for narrowing the *d* bands that avoids the Jahn-Teller effect and classical orbital ordering. Such SOC-induced band narrowing enhances the effects of electronic correlations leading to a new form of insulator called a spin-orbit Mott insulator[75]. In both the weakly- and strongly-interacting regimes, SOC entangles spin and orbital degrees of freedom and enhances multipolar correlations, producing highly anisotropic two-site interactions. The latter is exquisitely sensitive to exchange topology[76]. However, very little has been probed experimentally in this area owing to the significant challenges associated with the growth of the relevant materials, the small size of the successful single crystals produced (~ few microns), and the limitations of the techniques available to probe such small samples.

The high coherent flux, nanometer beam size and the full polarisation control delivered by the CSXID beamline, in the tender X-ray range close to 3keV, offers an exciting opportunity to perform state-of-the-art 3D imaging that can reveal the nature of the electronic and magnetic correlations that endow these materials with their novel properties. An interesting example to be explored are the Ruthenates, which show myriad novel complex properties ranging from the metal-insulator transition (MIT)[77,78], AFM ordering[78,79], weak ferromagnetism[80], orbital ordering[81] and a complex modulated order mediating a spin reorientation transition (SRT) [Ref. 82]. Coherent X-rays can directly probe the order parameters, the collective dynamics and the real-space information of the domain structures formed in the vicinity of a phase transition. Moreover, Bragg Coherent Diffraction Imaging (BCDI) can benefit from the extended Ewald sphere provided by the 4*d* *L*-edge energies to access distinct Bragg peaks. In turn, this can lead to real-space maps, via iterative phase retrieval algorithms, of the internal strain behind the structural phase transition that usually accompanies a MIT or SRT. A system of note is Ca_2RuO_4, where the spatial organisation and dynamics of the electronic and magnetic phase separation are expected to play a dominant role in its physical properties. A bulk-sensitive, 3D nanoprobe such as nanoDiffraction Imaging or BCDI will provide a comprehensive map of the structural, electronic and magnetic phase-separation allowing the complexity of the phase diagram to be disentangled for the first time.

3.2.4 Energy materials

Electrochemical energy storage is critical to the decarbonisation of the UK economy to meet ambitious net-zero emissions commitments aimed at mitigating climate change. Rechargeable batteries, particularly those based on Li-ion technology, are already widely deployed in portable electronics and increasingly for vehicle electrification. The electric vehicle battery industry, estimated to be worth £2.7 billion per year by 2030, will benefit from the insights the CSXID beamline will be able to provide into the performance of new solid electrolyte materials and low cost, high energy density electrodes. This will involve key users from the Faraday Institution which brings together national expertise in this area and is headquartered on the Harwell Campus.

As identified by the Faraday Institution, more widespread adoption of rechargeable batteries in areas such as grid-scale storage for intermittent renewable energy sources, requires further increases in energy density and reductions in cost. The electrodes used are typically composites consisting of microparticles of the active materials, embedded in conductive additives, and polymeric binders. Developing new high-energy density and low-cost materials that retain their capacity over thousands of charge-discharge cycles, increasingly requires understanding of spatial heterogeneity in both the reversible redox processes occurring in the active materials and the unwanted degradation reactions

occurring throughout the electrode particularly at interfaces[83]. This is particularly the case for cathode materials based on $LiNi_xMn_yCo_zO_2$ (NMC) chemistry that have entered the market, and where over the coming decade, the increase the Ni content is expected to improve capacity and reduce the content of costly Co. However, this also increases the surface reactivity of these materials, leading to severe degradation through side reactions including transition metal dissolution, electrolyte decomposition, and irreversible changes in the phase of the NMC. The unprecedented spatial resolution and chemical contrast offered by the CSXID beamline for both transition metals as well as light elements will be invaluable in locating and understanding the origins and progress of these degradation processes.

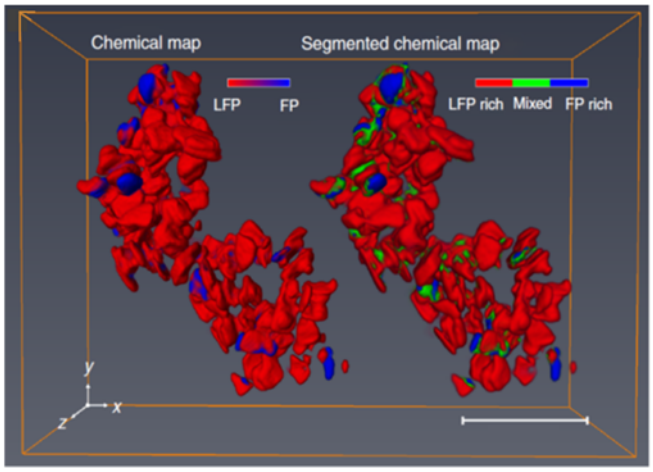

Figure 3 3D chemical map and its segmentation into three chemical phase groups. The presence of the $Li_\alpha FePO_4$ (majority Fe^{2+}, LFP) and charged $Li_\beta FePO_4$ (majority Fe^{3+}, FP) are assigned as red and blue, respectively (left). The voxels are separated into three distinct groups, indicating chemical phase group of each voxel. The red, green, and blue areas indicate LFP-rich (>70% $Li\alpha FePO_4$), FP-rich (>70% $Li_\beta FePO4$), and mixed (30–70% $Li_\alpha FePO_4$, the rest being $Li_\beta FePO_4$) domains, respectively. The scale bar is 500 nm. See Ref. 84 for details.

Access to the light elements, precluded using hard X-rays on I14, prevalent in battery electrolytes will allow interface degradation to be detected, particularly the nature of the thin (5-50 nm) solid- and cathode-electrolyte interphases (SEI/CEI) formed. The ability to reveal differences between the inorganic and organic species formed at different facets of the active NMC particles will help inform the design of the active material morphology including “single-crystal” NMC materials where only certain facets are exposed. It will also be possible to determine how transition metal species dissolved from the cathode influence the graphite anode. This could include their role in undesired thickening of the SEI, as well as whether they continue to exhibit redox behaviour when embedded in the SEI [Ref. 85].

Spatially resolving transition metal and anion (*e.g.* Oxygen) redox will also be invaluable for understanding the performance and stability of novel cathode materials, such as Li-rich layered-oxide cathodes that offer further improvements in capacity[86,87]. In particular, this will reveal the extent to which redox occurs uniformly within individual cathode particles (see Figure 3) and across the population of particles that make up the composite electrodes, particularly at high cycling rates,[84] as well as the formation of any surface reconstruction layers that may help stabilise these materials[87]. This could be used to probe the effectiveness of cathode materials with core-shell or graded-stoichiometries, both in reversibly storing charge and also supressing irreversible side-reactions at the surface of the cathode particles.

Although Li-ion chemistry is commercially established, the CSXID beamline is expected to help progress the full range of emerging chemistries (Na/K-ion, multivalent ions, metal-air, redox flow *etc.*). For example, in the field of solid-state electrolytes for sodium-metal batteries, it would provide powerful spatiochemical imaging at the interface between the metal electrode and novel sulfide electrolytes[88], revealing dendrite penetration at defects such as grain boundaries and the chemical impacts of this. The ability to perform these measurements *in situ* will help accelerate progress in developing these materials, beyond the limited resolution post-mortem imaging (*e.g.* Secondary ion mass spectrometry) currently applied.

3.2.5 New frontiers in catalytic science

Supported catalysts represent a major form of heterogeneous catalysis in a market estimated to be worth $34 billion per annum. These catalysts typically comprise precious group metals/metal oxides supported on a refractory oxide. It is well known that the right combination of active metal and support can lead to significant improvements in catalytic performance (in terms of activity, selectivity, lifetime and atom efficiency). However, the subtleties between a good catalyst and a great one remain poorly understood. In recent years the increasing availability of nano and atomic imaging capabilities at synchrotrons sources has led to something of a renaissance in our ability to probe and understand these subtleties; in particular the probing of the interface between the metal nanoparticle and the support[89]. This frontier has largely been suspected of playing a significant role in catalytic performance yet its importance has largely been inferred by bulk measurements or else approximated by theory. Some very recent and exciting studies have shown how similar beamlines (*e.g.* COSMIC) are now able to visualise single metal nanoparticles and to determine (often under relevant *in situ* conditions) the spatial distribution of their physico-chemical properties thereby identifying what makes the interfacial structure/behaviour so important[90]. The next generation CSXID beamline with better spatial resolution will play an essential role in the characterisation of 'frontier' catalytic materials *i.e.* those containing single-(metal)atom/ion and clusters[91]. Although these materials have garnered much interest over the past 5-10 years, these catalysts pose a challenge in terms of their characterisation, being limited to HRTEM studies which are only able to identify the presence of the species. The chemical nature then remains poorly understood since the spatial resolution of current element specific X-ray imaging techniques is not good enough at present. In addition, the possibility to perform spectroscopic measurements at multiple edges allows the physico-chemical behaviour of both metal and support to be determine simultaneously, allowing for a more complete understanding of the processes involved. This has the potential to revolutionise the entire field of supported catalysts particularly at a time when there is a demand for efficiency improvements (in terms of their manufacture and their performance) and sustainability.

Redox catalysis, where electron transfer controls reaction pathways, nowadays relies on quantum confinement which radically alters the nanoparticle electronic structure leading to considerable enhancements in reactivity[92]. More generally, it has long been debated whether reactions occur on or around a supported metal nanoparticle so that element-specific nanoimaging studies at the perimeter of nanoparticles as well as on top using an AC-PEEM would be ground-breaking. Candidates could be noble metal particles on surfaces or enclosed in carbon nanotubes. Spectromicroscopy on the CSXID beamline with ≤10nm resolution is an ideal tool with which to image adsorption and reaction on facets, using the variable temperature of the instrument to control the reaction rate. Observing increased reaction rates through a multiwalled carbon nanotube filled with noble metal nanoparticles or increased reactions rates on a single nanowire or nanoparticle would be revolutionary. For instance, for supported Pd nanowires, one might expect high activity at the curved tips or kinks which could be followed in real time at high resolution. Photocatalytic applications using ~40nm nanoparticles deposited on TiO_2 have been proposed to act as plasmonic antennas[93] or as electron sinks if smaller. Larger nanoparticles could be activated with a visible laser and the reactivity (to *e.g.* ethanol) around the nanoparticle investigated with size in real time using the rapid 3D tomography made possible by the huge increase in coherent flux on the CSXID beamline.

3.2.6 Controlling emergence using phase separation

Quantum materials often exhibit rich phase diagrams arising from the subtle interplay among the charge, spin, orbital and lattice degrees of freedom. For example, an anomalous conducting phase can emerge in correlated insulators or Mott insulators through a temperature change or chemical doping. In such a correlated metal, the mobile charges experience strong competing interactions leading to exotic phases, including the pseudogap state in cuprates and manganites, high-temperature superconductivity, charge density waves in cuprates, and even phase separation in some manganites and cuprates. Here,

nanoDiffraction Imaging and BCDI will uncover the details of the phase separation and percolation during phase transitions giving detailed microscopic insights in macroscopic quantities such as resistivity[94] and coercivity. With an upgrade to Diamond-II, the reduction of the horizontal beam size and divergence will allow spatially-resolved Resonant Inelastic X-ray Scattering (RIXS) on the nanoscale (nano-RIXS) on I21 with the possibility of mapping the dynamic structure factor of quantum materials in real space to trace the origin of emergent phenomena opening up the possibility of engineering new materials with technologically relevant properties. The combination of BCDI on the CSXID beamline and nano-RIXS on I21 would then give detailed insights into the influence of strain and confinement on the excitations present in a host of quantum materials.

To understand and manipulate the microscopic mechanisms leading to emergent phenomena such as superconductivity, magnetoelectric coupling and magnetism it is imperative to decode phase fluctuations with nanometer spatial resolution. X-ray Photon Correlation Spectroscopy (XPCS) is envisaged to play an increasingly important role since it probes the dynamical structure factor in the time domain. The scattering wavevector the gives the spatial correlations. Currently, microsecond dynamics, on length scales of hundreds of nanometres to several Ångstroms, can be accessed using third-generation sources. The large increase in coherent flux on Diamond-II will then allow the possibility of fast (MHz) dynamics to follow spatial correlations probed on much smaller length scales for an array of materials. For instance, magnetic skyrmions are considered to be stabilised by spin fluctuations arising from the competition between the symmetric and antisymmetric exchange interactions giving rise to disordered phases with skyrmion-like short range order close to the ordering temperature in MnSi [Ref. 95] . Element-resolved XPCS would give transformative insights into the dynamics of skyrmion formation and the relevant order parameters. XPCS would also make a huge impact on the understanding of nanoscale phase separation in quantum materials, which has the potential to create devices based on new emergent phenomena.

3.3 Diamond-II portfolio

The CSXID beamline will be a unique addition to the Diamond-II portfolio, taking advantage of the large increase in coherent flux to generate a step change in the nanoscale 3D imaging capabilities available to UK science and industry. Polarised X-ray 3D imaging, with nanoscale resolution, is not currently available at Diamond, yet significant advances have been made with stunning recent 3D studies at large-scale facilities. The Magnetic Materials Group has identified key areas of activity in a 10 year plan, including the development of strain and electronic imaging using BCDI on I16, high-resolution chemical and magnetic imaging using Aberration-Corrected PEEM (AC-PEEM) on I06, mapping excitations in phase separated quantum materials using nano-RIXS on I21 and depth profiling spin textures using XMCD on I10. The new capabilities of the CSXID beamline will be pivotal to gaining new multidisciplinary insights into the fundamental phenomena determining the performance of new materials and devices. The diffraction branch of the CSXID beamline will further have synergies with the scattering branch of I06 and I10.

The CSXID beamline links directly to activities of I13, I14 and J08. The CSXID beamline will complement I13 and I14 by giving imaging access to lighter elements using soft X-rays which is more challenging for hard X-rays. The CSXID beamline will be complementary to J08, focussing on a different energy range and sample environments. The J08 beamline has an energy range of 250-2000eV and focusses on imaging at the *C*, *N*, and *O* K-edges with sample environments dedicated to biological samples and polymer science. The CSXID beamline, on the other hand, will cover a broader energy range (250-3000eV) and will be developed to achieve cryogenic temperatures, magnetic fields, fast pulsing and *operando* reaction cells with the timing infrastructure to perform ultrafast experiments on the picosecond timescale. The capabilities of the CSXID beamline are directly related to the ultrafast insights that can be gained at the ARTEMIS facility at the CLF or new XFEL facilities coming online. Synergies between the catalysis hub and the CLF imaging centre, based at the Research Complex at Harwell (RCaH), are also relevant. A central axis of activity of the CSXID beamline will be the development of advanced sample environments with the aid

of the existing facilities available at the Harwell Campus which include the ISIS sample characterisation laboratory and the FIB instruments available at Diamond and the RCaH.

3.4 Academic user community and beneficiaries

There is a substantial user community that will benefit directly from the 3D magnetic and chemical imaging capabilities of the CSXID beamline, from those researchers working on quantum materials to energy storage to those developing new and novel nanostructured devices using advanced 3D printing techniques. The CSXID beamline proposal received **188** statements of support (of which 50% are from the UK; see section 7 and Appendix A) from research communities working in diverse areas such as spintronics, complex oxides, catalysis, battery materials and quantum materials.

Coherent X-ray imaging will provide element-selective 3D scalar and vector mapping with nanometer scale spatial resolution transforming many fields by permitting the mapping of, for instance, the position, velocity and chirality of novel spin textures that are controlled by spin-polarised currents and magnetic and electric fields. The element-specific 3D tracking of electrochemical reactions in battery materials along with electrode degradation, as well as chemical mapping of functional catalytic materials, will become routinely available on the CSXID beamline benefitting both existing academic and industrial researchers working with well-established hard X-ray probes. The *ultrafast* 3D imaging capabilities, at low-temperatures and high magnetic and electric fields, will provide opportunities for step changes in our understanding of how nanoscale phenomena control macroscopic properties in quantum materials. These latter advances build expertise relevant for the free-electron laser facilities currently being proposed and built. Key beneficiaries are the UK-based magnetism, catalysis and energy materials research communities and with the time to generate a full 3D chemical or magnetic tomogram falling from ~1day for the first results to ~2 hours at the CSXID beamline, the possibilities will then expand dramatically.

3.5 Industrial user community and beneficiaries

The new capabilities available at the CSXID beamline (*e.g.* 3D chemical and magnetic contrast, high spatial-temporal resolution, spectromicroscopy of light and heavy elements) will address challenges in developing functional and quantum materials to fill gaps in understanding the behaviour of complex, real-world materials *e.g.* the behaviour of materials at interfaces and the inter-dependency of their properties with microscopic composition. The research output of the CSXID beamline will be relevant across a number of sectors[f] including energy, automotive, electronics, information and communication and manufacturing.

Maximising the impact of research for the benefit of UK plc requires publicly funded, multidisciplinary teams of scientists and high levels of collaboration between academia and industry working on state-of-the-art facilities such as the CSXID beamline. The sample environment development laboratory will specifically address the challenges faced by industry in accessing soft X-ray beamlines with the aim of making *operando* measurements using TEM sample holders standard. The CSXID beamline will also enhance the collaborative and strategic partnerships between academia and industry which are crucial for the two-way flow of knowledge. Two mechanisms for industry to use beamtime at Diamond are through the Industrial Liaison Office or through companies (*e.g.* Finden Ltd.) capable of bridging the link between academic and industrial research by providing advanced characterisation and expert analysis to derive structure-activity relationships in functional materials under operating conditions for clients. For companies like Finden Ltd., the CSXID beamline will provide an opportunity to exploit new data processing capabilities for large volume data screening. The huge decrease in data acquisition time will allow more attractive pricing models for the industrial user base with 3D imaging possible with one or two hours of beamtime. The development of unique, fast and automated magnetic and chemical imaging tools at the CSXID beamline, to explore material performance under real operating conditions and at high spatial resolution in 3D, will then attract many researchers from international companies. A number of statements of support from industry (Johnson Matthey, WesternDigital, Seagate, Hitachi, SABIC, Finden Ltd.) have indicated a need

[f] https://epsrc.ukri.org/newsevents/pubs/the-economic-benefits-of-chemistry/

for high-resolution 3D imaging to advance the development of future data storage devices, energy materials and catalysis (see section 7).

3.6 Comparison to other synchrotron facilities, current and planned

There is no capability in the UK for X-ray vector tomography that can reveal the details of new and novel emergent properties of functional and quantum materials in 3D. There is no capability in the UK to study the picosecond dynamics of novel spin textures, such as skyrmions and chiral domain walls using the high spatial resolution of 3D X-ray imaging. There is no capability in the UK to map the multiple reaction points and heterogeneity of energy materials in 3D or to probe the reaction centres on catalytic nanoparticle surfaces using the strong resonances available in the soft X-ray range. There is no capability in the UK to improve the performance of battery materials using insights gained via a unique and powerful probe of lighter elements such as soft X-ray 3D tomography. If the *status quo* is maintained then the research community will have access to J08 (a branchline of I08 with 50% of the beamtime) and dedicated to imaging of biological samples, polymers and minerals with detectors optimised for the *C*, *N* and *O* K-edges. Alternatively, the UK community could make use of facilities available overseas at the ALS, SLS, ALBA, NSLS-II, SOLEIL and BESSY, but this may severely hinder research involving preparation of complex samples that are not readily transportable (*e.g*. batteries).

The CSXID beamline will comprise one branchline for imaging in transmission, using ptychography or STXM, and one branchline for soft X-ray diffraction and scattering combined with nanoscale imaging as well as developing XPCS. The performance parameters of the CSXID beamline are compared to existing facilities in Table 1. The exact beam size will balance coherent flux and the focussing requirements of the two CSXID branches and will be the subject of a detailed Conceptual Design Review (CDR). In the present study, a 20nm spot size is assumed as the requirement for both branches with ptychography being performed out of focus with a larger spot size. The use of high-efficiency multilayer gratings (MG), produced in the new Diamond Multilayer Fabrication facility, would further increase the coherent flux.

We emphasize that Table 1 compares contrast and throughput gains compared to COSMIC and MAXYMUS, which are operational beamlines with world-leading *current* capabilities in 3D tomography and time-resolved magnetic and chemical imaging. We have included the performance of J08 which will start operations as a user facility in 2021. We note that SOFTIMAX is coming on line at MAXIV and has a similar performance to J08. There will be some overlap between the CSXID beamline and J08, but the overlap in scientific activity is much closer to COSMIC and MAXYMUS. The COSMIC beamline is planning to have a comparable flux to the CSXID beamline after the ALS-U upgrade with a new 4m insertion device.

	COSMIC	MAXYMUS	J08	**CSXID (Long)**	CSXID(Mid)
Source	UE36 (2m)	UE36 (3.2m)	UE53(4.5m)	**UE56(5m)**	UE56(1.8m)
Energy Range	250-2500eV	130-2500eV	250ev-2000eV	**250-3000eV**	250-3000eV
Coherent flux@sample	1e9 1e12(ALS-U)	1e9	6e10 2e11 (DII)(MG)	**7e11** **2e12(MG)**	6e10 2e11 (MG)
Resolving Power	3000	3000	5000	**8000**	7000
Beam@ZP	ϕ = 0.75mm	1.8mm (H) 1.6mm (V)	1.86mm (H) 0.29mm (V)	**0.32mm (H)** **0.25mm(V)**	0.53mm(H) 0.37mm(V)
Beam@sample	55-200nm*	30-125nm*	70nm*	**20 - 500nm***	20-500nm*
Spatial resolution	11nm	12nm	8nm	**<10nm**	<20nm
Contrast	x1	x1	x8	**x25**	x6
Throughput	x1	x1	X60	**x700** **x2000*(MG)**	X60 x200* (MG)

Table 1 Comparison of the performance parameters of the CSXID beamline in the long and mid-straight sections with J08 (the I08 branchline), COSMIC[96] at the ALS and MAXYMUS[97] at BESSY. The beam parameters are given for 500eV. * Ptychography can be readily performed out of focus [98].

4. Beamline performance specification and requirements

The increase in coherent flux (*F*) on Diamond-II will lead to two significant advantages for nanoscale 3D imaging, namely a substantial increase in *throughput*, and an increase in the achievable *spatial resolution*. The time to record a 3D tomogram at a constant spatial resolution scales linearly with *F*, assuming on-the-fly scanning. For 3D imaging[99], the spatial resolution (Δx) improves with the fourth root of the flux $\Delta x \sim \sqrt[4]{F}$ and the contrast improves as $\sqrt{F}$, which is crucial when measuring low dichroic signals using polarised X-rays. To quantify the effect of the increase in coherent flux on the measurement time and spatial resolution, we consider the relationship of the fundamental components of 3D imaging, assuming that the X-ray source is stable, the sample does not degrade and the detector does not introduce noise. We quantitatively compare the relative (*cf.* MAXYMUS, COSMIC, *F*=1e9) change in Δx and T for different *F* in Figure 4. We see that, even with a conservative 5% overhead (Figure 4b), significant increases in throughput and the spatial resolution are possible on the CSXID beamline.

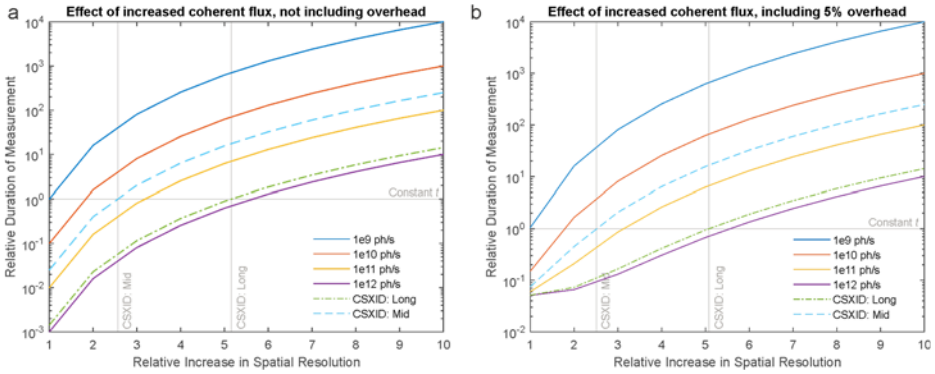

Figure 4 Influence of the increase in coherent flux on the measurement time for different spatial resolutions. The relative measurement time is given for different increases in spatial resolution for a range of coherent flux assuming a) negligible overheads and b) assuming a 5% overhead.

4.1 Additional developments required

The CSXID beamline will combine high-resolution coherent imaging with a state-of-the-art sample sample environment development laboratory, which will enable the imaging of nanoscale features in 3D under *operando* conditions. Furthermore, new sample geometries and time-resolved techniques will be key to the capabilities of the CSXID beamline and are addressed below.

4.1.1 3D imaging with laminography

The principle of 3D imaging techniques is that a set of high-resolution 2D projection images are measured around a rotation axis (see Figure 5), and the internal 3D structure is recovered with a reconstruction algorithm. While for cylindrical samples, the tomographic geometry is an effective imaging technique, for flat, extended samples (*e.g.* Si_3N_4 membranes) certain angles are blocked, leading to artefacts in the reconstruction. The laminography geometry offers significant advantages in that the effective thickness of the sample remains constant for all projections. Ptychographic laminography will be implemented at the CSXID beamline following implementation at the cSAXS and Pollux beamlines at the SLS, where ultra-high precision ptychographic imaging around a rotation axis has been performed. A 60° tilt of the laminography rotation axis, to the X-ray beam, has been demonstrated to offer high accuracy 3D electronic[14,15] and magnetic[12] imaging. For magnetic vector laminography, XMCD images are measured over 360° about the rotation axis. The resulting 3D magnetisation vector field reconstructed using a tailored iterative reconstruction algorithm[12,100], has been combined with pump-probe measurements to map coherent rotation modes and domain wall dynamics[12]. A significant current limitation of 3D measurements concerns the measurement time (>>1week) meaning that such studies are not yet feasible for much of the user community. With the increased coherent flux of the CSXID beamline, *operando* 4D imaging will become routine, meaning that new opportunities arise for a wide range of disciplines.

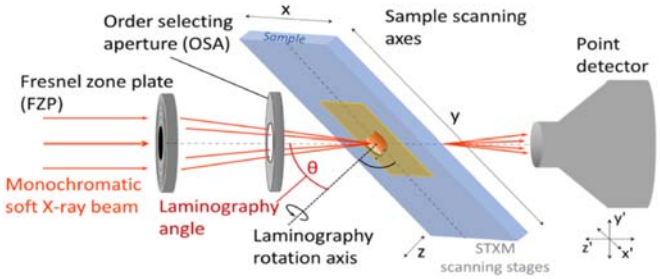

Figure 5 Soft X-ray laminography imaging geometry, in which xyz denotes the sample coordinate system and x'y'z' denotes the X-ray microscope coordinates. The laminography axis of rotation is at an angle, θ , to the x-ray beam. See Ref. 14 for details.

4.1.2 3D imaging of dynamics

Time-resolved imaging, where a pump signal is frequency and phase-matched to the synchrotron time structure will be available on the CSXID beamline. Such pump-probe imaging has recently been demonstrated for ptychographic 3D imaging of magnetisation dynamics with laminography[12] . The high coherent flux of the CSXID beamline, will then offer high-resolution mapping of a range of 3D dynamics from topological structures, to coherent rotation modes of the magnetisation with a temporal resolution of ~100 ps. We will also implement time-resolved STXM (TR-STXM) that make use of fast photon-counting electronics to detect the X-ray pulses, separated only a few nanoseconds[71], to probe MHz and GHz dynamics (Figure 6).

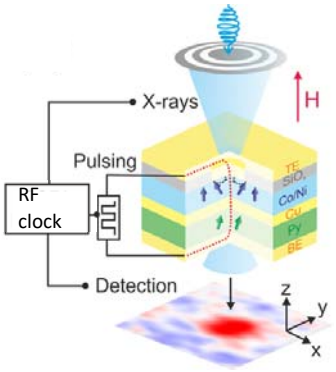

Figure 6 TR-STXM of a localised spin-wave (see Ref. 106 for details).

5. Schematic outline of the beamline

The beamline will comprise two branches, each covering an energy range from 250-3000eV, with complete control of the X-ray polarisation. One branch will be dedicated to transmission coherent imaging and STXM and the other to coherent imaging in reflectivity and scattering geometries. The coherent scattering branch will be versatile enough to allow the development of XPCS with the user community. The beamline will house a state-of-the-art sample environment development laboratory in order to take full advantage of the huge increase in coherent flux available due to the Diamond-II upgrade.

5.1 Source

For the Diamond-II upgrade, the ring energy will increase from 3 GeV to 3.5 GeV, and the electron beam emittance will be reduced from 2.7×10^{-9} m to 1.6×10^{-10} m. The insertion device (ID) for the CSXID beamline could be located either in a mid-straight section or a long-straight section. The maximum ID length for the mid-straight section is 1.8m, in contrast, it can be increased up to 5m for the long-straight section. Table 2 shows that the horizontal photon source size for both straights is very similar, while the vertical beam size for the mid-straight section is smaller due to the smaller β-function. In the soft X-ray range, the source size and divergence are limited by the photons rather than the electrons. Table 2 indicates that the photon beam divergence is inversely proportional to the square root of the undulator length (L) so the beam divergence for the mid-straight section is ~ 50% larger. As a result, this will decrease the beam footprint on the mirror and reduce the mirror length for the long-straight option. The smaller beam divergence for the long-straight means that the coherent flux at the sample will be ~12 times higher with the concomitant reduction (x12) in data acquisition time or improvement in spatial resolution (~ x2). The long-straight sections gives a coherent flux that would be impossible to achieve on the mid-straight section.

	ID L (m)	β_x (m)	β_y (m)	η_x (m)	Σ_x(μm)	Σ_y(μm)	$\Sigma_{x'}$(μrad)	$\Sigma_{y'}$(μrad)
Mid	1.8	2.340	1.920	0.025	32.1	8.5	27.1	26.4
Long	5.0	8.900	4.070	0.000	37.6	13.8	16.3	15.8

Table 2 CSXID beamline source parameters : ID length (L), β-function (β_x, β_y), horizontal dispersion function (η_x), photon source size (Σ_x, Σ_y) and divergence ($\Sigma_{x'}$, $\Sigma_{y'}$) for the mid and long straight section at 500 eV.

5.2 Optics

Two branches are required in this beamline, and the schematic of the proposed beamline is shown in Figure 7. The optical design of the beamline is based on a collimated plane grating monochromator (cPGM), which has many attractive features including the full flexibility of using it in many operational modes (high photon-energy mode, high spectral-resolution mode or high-harmonic suppression mode). Diamond has developed excellent experience in designing, building and operating cPGMs for many soft X-ray beamlines, such as I06, I10 and I09, I05, B07 and I08/J08.

The soft X-ray radiation delivered by the undulator is first collimated vertically by a cylindrical collimating mirror. The light is then dispersed vertically by a plane mirror and plane grating mirror. The beam is diverted into either branch by switching a cylindrical focusing mirror, which focuses the beam vertically onto the exit slits. In the horizontal direction, the light is only focused by an elliptical mirror to the exit slit, and it delivers a stigmatic image of the source at a monochromator exit slit for both branches.

One of consideration of the optical design of a microscopy beamline is to match the phase-space dimensions (full width and full angular width of the X-ray beam in x and y) to the microscope sample for which we have *desired* phase-space dimensions. Now the width-angular-width product of a synchrotron radiation beam is known as its phase-space area or emittance. Similarly, the phase-space area that can be accepted by a microscopy beamline achieving its diffraction-limited resolution is known as its acceptance.

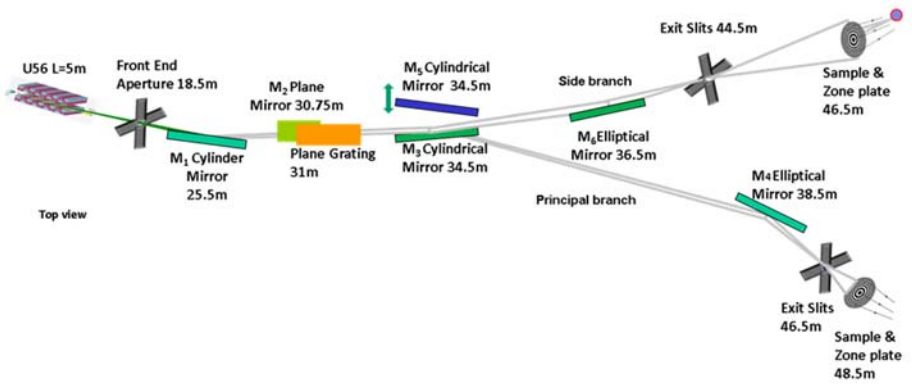

Figure 7 The optical layout of the CSXID beamline showing the imaging and scattering branch.

Usually, the emittance of a synchrotron X-ray beam does not match the acceptance of a microscopy beamline so that either the desired width or angular width of the X-ray beam arriving at the sample (or both) will be under/over filled.

The beam size and divergence for 500eV have been summarized in Table 2. The desired beam size at the exit slit is 10μm(H) x 10μm(V), and the divergence is 125μrad in both directions according to the known zone plate (ZP). The horizontal and vertical source size (FWHM) are around 88μm and 32μm, repectively, which can be achieved by using moderate focusing mirror and adjusting the beamline vertical magnification using the PGM parameters. Based on the above considerations, the beamline layout has been optimized to fully illuminate the ZP and achieve the maximum coherent flux. A fixed position of the end-stations relative to the secondary source will dramatically limit the full performance of the instrument in terms of secondary source demagnification and photon flux and coherence requirements over the entire 250-3000 eV photon energy range. Thus, it is suggested to adapt the secondary source to ZP distance by about 1-4 m by precisely movable support mechanisms of the end-station. The use of fully coherent illumination for diffraction-limited operation is a trade-off with the spatial angle that the ZP accepts. In many cases, it will be useful to overfill the ZP for stability reasons. We note that gains in coherent flux are possible if stable wavefronts can be achieved using focussing mirrors which will be explored during the CDR.

5.3 End-stations for the two branchlines

The end-stations for both branchlines will house a ZP to form a coherent illumination spot on the sample of the order of 20nm in diameter with the diffraction patterns recorded using accurately encoded sample positions over a region of interest of several microns. A differential interferometer scheme will be used to measure the ZP lens with respect to the sample in x and y. The redundancy required for robust numerical reconstructions will be provided by overlapping the illumination between successive exposures. Ptychographic images will be reconstructed in this way at each orientation for tomography, with transverse registration between views limited by the precision of the sample chuck. A full technical design will optimise the illumination geometry and detector pixelation, along with the most efficient scanning scheme. A key feature of the imaging end-station will be the high vacuum enabling cryogenic temperatures (<20K) at the sample and electrical connections allowing high-frequency pulsing. As detailed in section 5.4, one of the main objectives of the proposal is to offer *operando* environments that are already available for TEM sample mounts. In this respect, we envisage a close collaboration with the national electron Physical Science Imaging Centre (ePSIC) at Diamond to develop and establish these facilities at the CSXID beamline. On the other hand, the diffraction end-station will be designed for NanoDiffraction Imaging, BCDI and XPCS with higher magnet fields (~1T) available and cryogenic sample temperatures (<20K). We envisage a custom designed diffractometer for coherent imaging and dynamic studies which would complement the advanced, versatile RASOR diffractometer on I10 designed for soft x-ray diffraction with polarisation analysis.

To make the most of the high coherent flux for higher spatial resolution, high dynamic range detectors will be required. The Percival collaboration[g] currently aims to provide the research community with a large pixelated detector, able to distinguish single photons in the soft X-ray regime with a large dynamic range and high frame-rates. The combination of challenges results in a unique detection system, particularly suited for photon science experiments in the soft X-ray range. The main energy range of the Percival detector also covers the transition metal *L*-edges vital for the fast-magnetisation studies envisaged for the CSXID beamline. A characterization of small-size prototypes of the Percival detector has been presented in the past[101]. Another possible solution is the MÖNCH hybrid silicon pixel detector based on charge integration and with analogue readout. Its design is optimized for the single photon counting regime and has a maximum frame rate of 6kHz.

5.4 Sample preparation facilities and accessing extreme conditions

The CSXID beamline will house a dedicated sample environment development laboratory to support the user community in preparing cutting edge experimental sample environments with characterisation facilities to take full advantage of the comprehensive imaging capabilities of the beamline. In addition, a focused ion-beam/ scanning electron microscope (FIB/SEM) is available at the ePSIC, the electron Bio-Imaging Centre (eBIC) and at RCaH. In these cases, thin sample slices can be prepared and transferred onto standard TEM sample supports for imaging on the beamline. For more complex devices, such as spin-torque oscillators fabricated in about 100 individual fabrication steps[102], post-fabrication of membranes using chemical etching will be possible in a wet processing lab. The facilities at ISIS, RCaH and the CLF, on the Harwell Campus, will underpin the structural, magnetic and chemical sample characterisation.

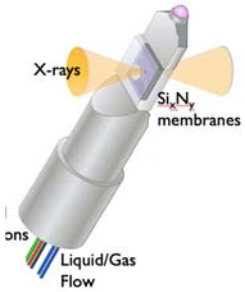

Figure 8 TEM style sample holder with a nanoreactor for *operando* studies.

The CSXID beamline will enable *operando* measurements in atmospheric pressure gas and liquid environments[103], combined with heating and electrical biasing capabilities[104]. A TEM-style holder will be specially adapted for this purpose with a mounting for interchangeable, MEMS-based silicon microchips (Figure 8). This technology is well established for electron microscopy and will help attract diverse research communities requiring the most challenging environments. A modular, exchangeable sample environment is envisaged, specialised for cryogenic temperatures as well as heating, fast-changing vector magnetic fields, and pulsed lasers in the visible regime, that will also accommodate the TEM-style holder. In particular, the branchline will be designed for research focussing on such extreme conditions including high fields and low temperatures.

5.5 Computing infrastructure and support

Ptychography is a computationally expensive imaging method and often requires many iterations before the phase retrieval algorithm converges to a high-quality reconstructed image. Therefore, a key ingredient for any ptychographic setup is a dedicated high-performance computing infrastructure and fast reconstruction codes. Over the past years, Diamond has invested in both which resulted in the development of a GPU-accelerated version of the ptychographic reconstruction software package PtyPy [Ref. 105]. Within the scope of projects at J08 (the ptychography branchline of I08), this GPU-accelerated ptychographic workflow has been successfully integrated into “Zocalo”, the automated processing infrastructure at Diamond. With the planned improvements of workflow pipelines, it should be possible to reduce the latency to just a few seconds by the time Diamond-II is built. Together with further advances in high-performance computing, the objective of providing researchers with fully-automated, real-time ptychographic 3D imaging becomes a reality. Access to the computing infrastructure will be equally important for advanced post-processing of 3D imaging datasets to achieve high-quality tomographic reconstructions of both scalar and vector fields after beamtime.

[g] A collaboration between DESY, STFC, ELETTRA, DLS, PAL and SOLEIL has developed the Percival detector.

6. References

1. Ade, H. & Stoll, H. Near-edge X-ray absorption fine-structure microscopy of organic and magnetic materials. *Nat. Mater.* **8**, 281–290 (2009).
2. Fischer, P. Magnetic imaging with polarized soft x-rays. *J. Phys. D. Appl. Phys.* **50**, (2017).
3. Bak, S. M., Shadike, Z., Lin, R., Yu, X. & Yang, X. Q. In situ/operando synchrotron-based X-ray techniques for lithium-ion battery research. *NPG Asia Mater.* **10**, 563–580 (2018).
4. Kazakova, O. *et al.* Frontiers of magnetic force microscopy. *J. Appl. Phys.* **125**, (2019).
5. Tripathi, A. *et al.* Dichroic coherent diffractive imaging. *Proc. Natl. Acad. Sci. U. S. A.* **108**, 13393–13398 (2011).
6. Luo, Z. *et al.* Chirally coupled nanomagnets. *Science (80-.).* **363**, 1435–1439 (2019).
7. Foerster, M. *et al.* Direct imaging of delayed magneto-dynamic modes induced by surface acoustic waves. *Nat. Commun.* **8**, 1–6 (2017).
8. Ghidini, M. *et al.* Shear-strain-mediated magnetoelectric effects revealed by imaging. *Nat. Mater.* **18**, 840–845 (2019).
9. Brown, W. F. Virtues and weaknesses of the domain concept. *Rev. Mod. Phys.* **17**, 15–19 (1945).
10. Gutfleisch, O. *et al.* Magnetic materials and devices for the 21st century: Stronger, lighter, and more energy efficient. *Advanced Materials* **23**, 821–842 (2011).
11. Donnelly, C. *et al.* Three-dimensional magnetization structures revealed with X-ray vector nanotomography. *Nature* **547**, 328–331 (2017).
12. Donnelly, C. *et al.* Time-resolved imaging of three-dimensional nanoscale magnetization dynamics. *Nat. Nanotechnol.* **15**, 356–360 (2020).
13. Donnelly, C. *et al.* Three-dimensional magnetization structures revealed with X-ray vector nanotomography. *Nature* **547**, 328–331 (2017).
14. Witte, K. *et al.* From 2D STXM to 3D Imaging: Soft X-ray Laminography of Thin Specimens. *Nano Lett.* **20**, 1305–1314 (2020).
15. Holler, M. *et al.* High-resolution non-destructive three-dimensional imaging of integrated circuits. *Nature* **543**, 402–406 (2017).
16. Lancaster, T. *et al.* Transverse field muon-spin rotation signature of the skyrmion-lattice phase in Cu2OSeO3. *Phys. Rev. B* **91**, 224408 (2015).
17. Stefancic, A. *et al.* Origin of skyrmion lattice phase splitting in Zn-substituted Cu2OSeO3. *Phys. Rev. Mater.* **2**, 111402 (2018).
18. Cortes-Ortuno, D. *et al.* Proposal for a micromagnetic standard problem for materials with Dzyaloshinskii-Moriya interaction. *New J. Phys.* **20**, 113015 (2018).
19. Wilson, M. N. *et al.* Measuring the formation energy barrier of skyrmions in zinc-substituted Cu2OSeO3. *Phys. Rev. B* **99**, 174421 (2019).
20. Birch, M. T. *et al.* Increased lifetime of metastable skyrmions by controlled doping. *Phys. Rev. B* **100**, 014425 (2019).
21. Franke, K. J. A. *et al.* Investigating the magnetic ground state of the skyrmion host material Cu2OSeO3 using long-wavelength neutron diffraction. *AIP Adv.* **9**, 125228 (2019).
22. Birch, M. T. *et al.* Real-space imaging of confined magnetic skyrmion tubes. *Nat. Commun.* **11**, 1726 (2020).
23. Birch, M. T. *et al.* Anisotropy-induced depinning in the Zn-substituted skyrmion host Cu2OSeO3. *Phys. Rev. B* **102**, 104424 (2020).
24. Loudon, J. C. *et al.* Do Images of Biskyrmions Show Type-II Bubbles? *Adv. Mater.* **31**, 1806598 (2019).
25. Song, K. M. *et al.* Skyrmion-based artificial synapses for neuromorphic computing. *Nat. Electr.* **3**, 148 (2020).
26. Zeissler, K. *et al.* Pinning and hysteresis in the field dependent diameter evolution of skyrmions in Pt/Co/Ir superlattice stacks. *Sci. Rep.* **7**, 15125 (2017).

27. Jaiswal, S. *et al.* Investigation of the Dzyaloshinskii-Moriya interaction and room temperature skyrmions in W/CoFeB/MgO thin films and microwires. *Appl. Phys. Lett.* **111**, 022409 (2017).
28. Reyren, N. *et al.* Skyrmions in magnetic multilayers: chirality, electrical detection and current-induced motion. *Spintron. X* **10357**, 1035724 (2017).
29. Buttner, F. *et al.* Thermal nucleation and high-resolution imaging of submicrometer magnetic bubbles in thin thulium iron garnet films with perpendicular anisotropy. *Phys. Rev. Mater.* **4**, 011401 (2020).
30. Moreau-Luchaire, C. *et al.* Additive interfacial chiral interaction in multilayers for stabilization of small individual skyrmions at room temperature. *Nat. Nanotech.* **11**, 731 (2016).
31. Zeissler, K. *et al.* Diameter-independent skyrmion Hall angle observed in chiral magnetic multilayers. *Nat. Commun.* **11**, 428 (2020).
32. Saha, S. *et al.* Formation of Neel-type skyrmions in an antidot lattice with perpendicular magnetic anisotropy. *Phys. Rev. B* **100**, 144435 (2019).
33. Finizio, S. *et al.* Deterministic Field-Free Skyrmion Nucleation at a Nanoengineered Injector Device. *Nano Lett.* **19**, 7246 (2019).
34. Lemesh, I. *et al.* Current-Induced Skyrmion Generation through Morphological Thermal Transitions in Chiral Ferromagnetic Heterostructures. *Adv. Mater.* **30**, e1805461 (2018).
35. Zeissler, K. *et al.* Discrete Hall resistivity contribution from Neel skyrmions in multilayer nanodiscs. *Nat. Nanotech.* **13**, 1161 (2018).
36. Finizio, S. *et al.* Thick permalloy films for the imaging of spin texture dynamics in perpendicularly magnetized systems. *Phys. Rev. B* **98**, (2018).
37. Woo, S. *et al.* Deterministic creation and deletion of a single magnetic skyrmion observed by direct time-resolved X-ray microscopy. *Nat. Electr.* **1**, 288 (2018).
38. Woo, S. *et al.* Current-driven dynamics and inhibition of the skyrmion Hall effect of ferrimagnetic skyrmions in GdFeCo films. *Nat. Commun.* **9**, 959 (2018).
39. Skoric, L. *et al.* Layer-by-Layer Growth of Complex-Shaped Three-Dimensional Nanostructures with Focused Electron Beams. *Nano Lett.* **20**, 184–191 (2020).
40. Fernández-Pacheco, A. *et al.* Three-dimensional nanomagnetism. *Nat. Commun.* **8**, 15756 (2017).
41. Hertel, R. Ultrafast domain wall dynamics in magnetic nanotubes and nanowires. *J. Phys. Condens. Matter* **28**, (2016).
42. Jungwirth, T., Marti, X., Wadley, P. & Wunderlich, J. Antiferromagnetic spintronics. *Nat. Nanotechnol.* **11**, 231–241 (2016).
43. Barker, J. & Tretiakov, O. A. Static and Dynamical Properties of Antiferromagnetic Skyrmions in the Presence of Applied Current and Temperature. *Phys. Rev. Lett.* **116**, 1–5 (2016).
44. Wadley, P. *et al.* Spintronics: Electrical switching of an antiferromagnet. *Science (80-.).* **351**, 587–590 (2016).
45. Ashida, T. *et al.* Isothermal electric switching of magnetization in Cr2O3/Co thin film system. *Appl. Phys. Lett.* **106**, (2015).
46. Bezencenet, O., Bonamy, D., Belkhou, R., Ohresser, P. & Barbier, A. Origin and tailoring of the antiferromagnetic domain structure in α-Fe2O3 thin films unraveled by statistical analysis of dichroic spectromicroscopy (X-ray photoemission electron microscopy) images. *Phys. Rev. Lett.* **106**, 1–4 (2011).
47. Zhou, X. *et al.* Magnetotransport in metal/insulating-ferromagnet heterostructures: Spin Hall magnetoresistance or magnetic proximity effect. *Phys. Rev. B - Condens. Matter Mater. Phys.* **92**, 1–5 (2015).
48. Zhang, P., Finley, J., Safi, T. & Liu, L. Quantitative Study on Current-Induced Effect in an Antiferromagnet Insulator/Pt Bilayer Film. *Phys. Rev. Lett.* **123**, 247206 (2019).
49. Chmiel, F. P. *et al.* Observation of magnetic vortex pairs at room temperature in a planar α-Fe2O3/Co

heterostructure. *Nat. Mater.* **17**, 581–585 (2018).
50. Salazar-Alvarez, G. *et al.* Direct evidence of imprinted vortex states in the antiferromagnet of exchange biased microdisks. *Appl. Phys. Lett.* **95**, 2009–2012 (2009).
51. Waterfield Price, N. *et al.* Coherent Magnetoelastic Domains in Multiferroic BiFeO3 Films. *Phys. Rev. Lett.* **117**, 1–5 (2016).
52. Wadley, P. *et al.* Current polarity-dependent manipulation of antiferromagnetic domains. *Nat. Nanotechnol.* **13**, 362–365 (2018).
53. Martin, L. W. & Rappe, A. M. Thin-film ferroelectric materials and their applications. *Nature Reviews Materials* **2**, (2016).
54. Alapan, Y., Karacakol, A. C., Guzelhan, S. N., Isik, I. & Sitti, M. Reprogrammable shape morphing of magnetic soft machines. *Sci. Adv.* **6**, (2020).
55. Manipatruni, S. *et al.* Scalable energy-efficient magnetoelectric spin–orbit logic. *Nature* **565**, 35–42 (2019).
56. Petrie, J. R., Jeen, H., Barron, S. C., Meyer, T. L. & Lee, H. N. Enhancing Perovskite Electrocatalysis through Strain Tuning of the Oxygen Deficiency. *J. Am. Chem. Soc.* **138**, 7252–7255 (2016).
57. Ahadi, K. *et al.* Enhancing superconductivity in SrTiO3 films with strain. *Sci. Adv.* **5**, 1–6 (2019).
58. Bae, S. H. *et al.* Integration of bulk materials with two-dimensional materials for physical coupling and applications. *Nat. Mater.* **18**, 550–560 (2019).
59. Hong, S. S. *et al.* Extreme tensile strain states in La0.7Ca0.3MnO3 membranes. *Science (80-.).* **368**, (2020).
60. Kum, H. S. *et al.* Heterogeneous integration of single-crystalline complex-oxide membranes. *Nature* **578**, 75–81 (2020).
61. Ghidini, M. *et al.* Perpendicular local magnetization under voltage control in Ni films on ferroelectric BaTiO3substrates. *Adv. Mater.* **27**, 1460–1465 (2015).
62. Hasan, M. & Kane, C. Colloquium: Topological insulators. *Rev. Mod. Phys.* **82**, 3045–3067 (2010).
63. Hsieh, D. *et al.* A tunable topological insulator in the spin helical Dirac transport regime. *Nature* **460**, 1101–1105 (2009).
64. Haldane, F. D. M. Model for a quantum hall effect without landau levels: Condensed-matter realization of the 'parity anomaly'. *Phys. Rev. Lett.* **61**, 2015–2018 (1988).
65. Chang, C. Z., Zhang, J., Feng, X., Shen, J. & Zhang, Z. Experimental observation of the quantum anomalous Hall effect in a magnetic topological insulator. *Science (80-.).* **340**, 167 (2013).
66. He, Q. L. *et al.* Chiral Majorana fermion modes in a quantum anomalous Hall insulator – superconductor structure. *Science (80-.).* **299**, 294–299 (2017).
67. Valenzuela, S. O. & Tinkham, M. Direct electronic measurement of the spin Hall effect. *Nature* **442**, 176–9 (2006).
68. Hirsch, J. Spin Hall Effect. *Phys. Rev. Lett.* **83**, 1834–1837 (1999).
69. Kukreja, R. *et al.* X-ray Detection of Transient Magnetic Moments Induced by a Spin Current in Cu. *Phys. Rev. Lett.* **115**, 096601 (2015).
70. Liu, C. *et al.* Robust axion insulator and Chern insulator phases in a two-dimensional antiferromagnetic topological insulator. *Nat. Mater.* **19**, 522 (2020).
71. Bonetti, S. *et al.* Microwave soft x-ray microscopy for nanoscale magnetization dynamics in the 5-10 GHz frequency range. *Rev. Sci. Instrum.* **86**, 1–9 (2015).
72. Schaffer, R., Kin-Ho Lee, E., Yang, B. J. & Kim, Y. B. Recent progress on correlated electron systems with strong spin-orbit coupling. *Reports on Progress in Physics* **79**, (2016).
73. Witczak-Krempa, W., Chen, G., Kim, Y. B. & Balents, L. Correlated quantum phenomena in the strong spin-orbit regime. *Annu. Rev. Condens. Matter Phys.* **5**, 57–82 (2014).
74. Kuschel, T. & Reiss, G. Spin orbitronics: Charges ride the spin wave. *Nature Nanotechnology* **10**, 22–24 (2015).

75. Kim, B. J. *et al.* Novel jeff=1/2 mott state induced by relativistic spin-orbit coupling in Sr2IrO4. *Phys. Rev. Lett.* **101**, 1–4 (2008).
76. Jackeli, G. & Khaliullin, G. Mott insulators in the strong spin-orbit coupling Limit: From Heisenberg to a Quantum Compass and Kitaev Models. *Phys. Rev. Lett.* **102**, (2009).
77. Jain, A. *et al.* Higgs mode and its decay in a two-dimensional antiferromagnet. *Nat. Phys.* **13**, 633–637 (2017).
78. Braden, M. & André, G. Crystal and magnetic structure of Magnetoelastic coupling and the metal-insulator transition. *Phys. Rev. B - Condens. Matter Mater. Phys.* **58**, 847–861 (1998).
79. Pincini, D. *et al.* Persistence of antiferromagnetic order upon la substitution in the 4d4 Mott insulator Ca2RuO4. *Phys. Rev. B* **98**, 1–9 (2018).
80. Dass, R. I., Yan, J. Q. & Goodenough, J. B. Ruthenium double perovskites: Transport and magnetic properties. *Phys. Rev. B - Condens. Matter Mater. Phys.* **69**, (2004).
81. Porter, D. G. *et al.* Magnetic anisotropy and orbital ordering in Ca2RuO4. *Phys. Rev. B* **98**, 1–15 (2018).
82. Sokolov, D. A. *et al.* Metamagnetic texture in a polar antiferromagnet. *Nat. Phys.* **15**, 671–677 (2019).
83. Wolf, M., May, B. M. & Cabana, J. Visualization of Electrochemical Reactions in Battery Materials with X-ray Microscopy and Mapping. *Chem. Mater.* **29**, 3347–3362 (2017).
84. Yu, Y. S. *et al.* Three-dimensional localization of nanoscale battery reactions using soft X-ray tomography. *Nat. Commun.* **9**, 1–7 (2018).
85. Wandt, J. *et al.* Transition metal dissolution and deposition in Li-ion batteries investigated by operando X-ray absorption spectroscopy. *J. Mater. Chem. A* **4**, 18300–18305 (2016).
86. Cui, C. *et al.* Structure and Interface Design Enable Stable Li-Rich Cathode. *J. Am. Chem. Soc.* **142**, 8918–8927 (2020).
87. Boivin, E. *et al.* The Role of Ni and Co in Suppressing O-Loss in Li-Rich Layered Cathodes. *Adv. Funct. Mater.* (2020). doi:10.1002/adfm.202003660
88. Hayashi, A. *et al.* A sodium-ion sulfide solid electrolyte with unprecedented conductivity at room temperature. *Nat. Commun.* **10**, (2019).
89. Qiu, C. *et al.* Direct observation of the evolving metal–support interaction of individual cobalt nanoparticles at the titania and silica interface. *Chem. Sci.* (2020). doi:10.1039/d0sc03113e
90. Yoo, M. *et al.* A tailored oxide interface creates dense Pt single-atom catalysts with high catalytic activity. *Energy Environ. Sci.* **13**, 1231–1239 (2020).
91. Wang, A., Li, J. & Zhang, T. Heterogeneous single-atom catalysis. *Nature Reviews Chemistry* **2**, 65–81 (2018).
92. Pan, X. *et al.* Enhanced ethanol production inside carbon-nanotube reactors containing catalytic particles. *Nat. Mater.* **6**, 507–511 (2007).
93. Mubeen, S. *et al.* An autonomous photosynthetic device in which all charge carriers derive from surface plasmons. *Nat. Nanotechnol.* **8**, 247–251 (2013).
94. Mattoni, G. *et al.* Striped nanoscale phase separation at the metal-insulator transition of heteroepitaxial nickelates. *Nat. Commun.* **7**, 1–7 (2016).
95. Pappas, C. *et al.* Chiral paramagnetic skyrmion-like phase in MnSi. *Phys. Rev. Lett.* **102**, 197202 (2009).
96. Shapiro, D. *et al.* Development of coherent scattering and diffractive imaging and the COSMIC facility at the Advanced Light Source. *J. Phys. Conf. Ser.* **425**, (2013).
97. Follath, R., Schmidt, J. S., Weigand, M. & Fauth, K. The x-ray microscopy beamline UE46-PGM2 at BESSY. *AIP Conf. Proc.* **1234**, 323–326 (2010).
98. Odstrčil, M., Lebugle, M., Guizar-Sicairos, M., David, C. & Holler, M. Towards optimized illumination for high-resolution ptychography. *Opt. Express* **27**, 14981 (2019).
99. Howells, M. R. *et al.* An assessment of the resolution limitation due to radiation-damage in X-ray

diffraction microscopy. *J. Electron Spectros. Relat. Phenomena* **170**, 4–12 (2009).

100. Donnelly, C. *et al.* Tomographic reconstruction of a three-dimensional magnetization vector field. *New J. Phys.* **20**, (2018).
101. Khromova, A. *et al.* Report on recent results of the PERCIVAL soft X-ray imager. *J. Instrum.* **11**, (2016).
102. Macià, F., Backes, D. & Kent, A. D. Stable magnetic droplet solitons in spin-transfer nanocontacts. *Nat. Nanotechnol.* **9**, 992–996 (2014).
103. Gu, M. *et al.* Demonstration of an electrochemical liquid cell for operando transmission electron microscopy observation of the lithiation/delithiation behavior of Si nanowire battery anodes. *Nano Lett.* **13**, 6106–6112 (2013).
104. Unocic, R. R. *et al.* Direct visualization of solid electrolyte interphase formation in lithium-ion batteries with in situ electrochemical transmission electron microscopy. *Microsc. Microanal.* **20**, 1029–1037 (2014).
105. Enders, B. & Thibault, P. A computational framework for ptychographic reconstructions. in *Proceedings of the Royal Society A: Mathematical, Physical and Engineering Sciences* **472**, (Royal Society, 2016).
106. Backes, D. *et al.* Direct Observation of a Localized Magnetic Soliton in a Spin-Transfer Nanocontact. *Phys. Rev. Lett.* **115**, 127205 (2015).

7. Expressions of interest and engagement

7.1 Support from the community

The CSXID beamline will improve our understanding of nanoscale material properties in a wide range of research areas that include catalysis, magnetic materials, quantum materials, energy materials and electronic engineering. The scientific advances enabled by the facility will be of interest to communities working in condensed matter physics, chemistry, photonics, material science and surface science as evidenced by the scope of the discussions at the CSXID webinar held on the 28th September 2020, attended by **103** researchers, as well as the **188** statements of support received. The statements cover are a range of disciplines and techniques with strong representation from catalysis (23 statements), energy materials (15), magnetism (97), time-resolved science (34), *operando* conditions (31) and advanced sample environment development (18).The support from industry and academia is presented in the Appendix A, but we summarise a few elements of the support below.

The statements of support from industry emphasize the impact that the CSXID beamline will have on different sectors and comment on the lack of capabilities in the UK to address crucial problems. Johnson Matthey, who are stakeholders in the ePSIC, have a considerable interest in energy materials and catalysis and state that "*Our belief is that in the next few years there will be a greater emphasis on utilisation of such imaging techniques for energy storage materials applications. JM [also] has multimillion-pound business interests related to supported metal nanoparticles. Such catalysts underpin our profitable automotive catalysis business, but also play important roles in many other catalyst areas. An improved understanding of these materials, in particular under operating conditions, at a variety of length scales is key to drive further improvements in our technologies.*" WesternDigital, a global data storage corporation, state that "*Realizing the CSXID beamline would be highly beneficial to develop materials for future data storage and computation and provide guidance for academic and industrial research groups working in this field. … One issue that we face is that modern memory cells have become so small, that it has become very challenging to study their static and switching behavior. The planned CSXID beamline will provide a higher resolution, but also a very high throughput, which is necessary to gain meaningful data on nanostructures that are often very fragile. It also allows to reduce electrical stress on devices.*" Another international data storage company, Seagate, states that "*..it allows to visualise magnetic configuration in the bulk of an actual device, which is impossible with any other technique.*" In addition, Hitachi state that "*time-resolved XMCD measurement would be a particular useful tool to study the dynamics of such systems.*"

The Faraday Institution has a major interest in the CSXID beamline and state that "*The Coherent Soft X-Ray Imaging and Diffraction (CSXID) instrument will be a particularly valuable new technique, using the improved parameters of the Diamond-II source to 3D image samples at significantly improved resolution, <10nm, including the imaging of light elements. Extending current Faraday [Institution] studies using hard X-ray nanoprobes into the soft X-ray regime will allow the light elements prevalent in electrolytes and the binders of composites electrodes to be imaged which has so far been unfeasible at Diamond.*" The National Physical Laboratory also state that "*… this new national capability will allow an advanced research in the area of emerging and advanced energy materials such as 3D electrochemical reaction mapping and 3D chemical speciation mapping and mesoscale diffusion in polymer films. There is currently no capability in the UK to map the multiple reactions points and heterogeneity of energy materials in 3D.*"

The science case in section 3 presents the new scientific opportunities offered by the CSXID beamline. However, the statements of support (see Appendix A) mention other possibilities for advanced research in a number of disciplines. One opportunity is that the imaging capabilities could be employed to make dynamic measurements of magnetic drug delivery nanoparticles 'on-a-chip' as recently there have been important developments on membrane based microfluidic devices, allowing them to be used in the soft X-rays range [see statement by Julio Criginski Cezar, Appendix A page 49]. Another is, that future industrial and economic activities will largely depend on electrochemical processes, just as the last industrial revolution was dominated by thermochemical processes. Understanding how electrocatalysis and its

relation to water splitting, carbon dioxide reduction, nitrogen reduction, ammonia formation and biomass conversion proceeds using the CSXID beamline will be the key to designing better systems and materials [see statement by Yagya N Regmi, Appendix A page 7]. Another opportunity ris elated to 2D materials which are proposed to host topological domain structures and a skyrmion lattice, and with the inclusion of 'twist' introduced in heterostructures of layered materials, more exotic phenomenon is expected [see statement by Safe Khan, Appendix A page 36].

7.2 Statements of support and engagement summary

Total number of statements of support: **188**

Key for statements in Appendix A	Declared field of research	Percentage of respondents
	Physics	46%
	Materials Sciences	37%
	Chemistry	10%
	Engineering & Technology	3%
	Information & Communication Technologies	2%
	Energy	2% *

***** a further 7% of statements in other categories discuss the development of energy materials

Respondent location	Percentage of respondents
UK	50 %
International	50 %

Type of organisation	Percentage of respondents
Academic*	83%
Government	10%
Industry	3%
Non-Governmental Organisation (NGO)	1%
Other	3%

*~30% of user research declares an industrial component as determined by the Diamond Industrial Liaison Office

Diamond user status	Percentage of respondents
Currently a user at Diamond	69 %
Not currently a user at Diamond	31 %

Engagement webinar summary
Date of webinar: Wednesday 28th October 2020
Number of attendees: 103

Attendee location	Percentage of attendees
UK	75 %
International	25 %